CHALMERS
UNIVERSITY OF TECHNOLOGY

Synthesis and photophysical characterization of a pH-sensitive quadracyclic uridine (qU) analogue

Chemistry–A European Journal
Research Article
doi.org/10.1002/chem.202303539
Chemistry Europe
European Chemical Societies Publishing
www.chemeurj.org

Synthesis and photophysical characterization of a pH-sensitive quadracyclic uridine (qU) analogue

Hoang-Ngoan Le[+],[a, b] Jagannath Kuchlyan[+],[a] Tom Baladi,[b] Bo Albinsson,[a] Anders Dahlén,*[b] and L. Marcus Wilhelmsson*[a]

Fluorescent base analogues (FBAs) have become useful tools for applications in biophysical chemistry, chemical biology, live-cell imaging, and RNA therapeutics. Herein, two synthetic routes towards a novel FBA of uracil named qU (quadracyclic uracil/uridine) are described. The qU nucleobase bears a tetracyclic fused ring system and is designed to allow for specific Watson-Crick base pairing with adenine. We find that qU absorbs light in the visible region of the spectrum and emits brightly with a quantum yield of 27% and a dual-band character in a wide pH range. With evidence, among other things, from fluorescence lifetime measurements we suggest that this dual emission feature results from an excited-state proton transfer (ESPT) process. Furthermore, we find that both absorption and emission of qU are highly sensitive to pH. The high brightness in combination with excitation in the visible and pH responsiveness makes qU an interesting native-like nucleic acid label in spectroscopy and microscopy applications in, for example, the field of mRNA and antisense oligonucleotide (ASO) therapeutics.

Introduction

Current developments in the field of RNA-based therapeutics including the mRNA vaccine against SARS-CoV-2 have attracted great attention and the groundbreaking work regarding the discoveries concerning the role and need of nucleoside base modifications in mRNA therapeutics by Karikó and Weissman was recently awarded the 2023 Nobel Prize in Physiology and Medicine. Moreover, studies on endosomal escape and cellular trafficking pathways of these exogeneous nucleic acid molecules are of fundamental interest and importance.[1] Such studies often utilize fluorescence as the readout and for this the nucleic acid of interest is generally labeled with external dyes such as cyanine dyes using SPAAC chemistry. This makes the trafficking of these large biomolecules visible under a fluorescence microscope even at very low concentrations.[2] An alternative approach, that has been used quite successfully by us and others, is instead to employ fluorescent base analogues (FBAs) as labels.[3] FBAs are structure-mimicking emissive analogues of the canonical DNA and RNA nucleobases that completely or to a large extent preserve their chemical and biological properties, such as base pairing, stacking, and protein recognition. These modified nucleoside bases are significantly smaller compared to, for example, cyanine dyes[4] and are typically uncharged. However, FBAs are commonly absorbing in the UV region with a considerably lower brightness compared to cyanine and similar dyes. Hence, a large effort is being made in the field to develop novel FBA which mimic their corresponding natural nucleobase at the same time as they have a more red-shifted absorption profile and increased brightness.

FBAs have become useful tools not only for understanding nucleic acid structure, dynamics, and protein interactions but also for nucleic acid imaging and biomedical applications.[5] 2-aminopurine (2AP; absorption maximum (λ_{max}) 303 nm, Figure 1), an adenine analogue reported by Stryer *et al.* in 1969, is the most used so far with a wide range of applications in nucleic acids research.[6] However, 2AP has lower base-pairing specificity compared to adenine which makes it less suited for, for example, fluorescence anisotropy and Förster resonance energy transfer (FRET) techniques.[5c,7] More recent developments of highly emissive analogues such as 8vG (λ_{max} 277 nm),[8] 8vA (λ_{max} 290 nm),[9] and the isomorphic RNA alphabet have expanded the applicability of FBAs in nucleic acids studies.[10] Among them, thG (λ_{max} 321 nm) represents an excellent guanosine mimic with a high quantum yield (QY) when incorporated into different DNA and RNA oligonucleotides.[11] As an excellent FBA, thG has found several applications such as in monitoring DNA conformational changes,[12] base flipping,[11b] DNA-protein interaction,[13] and cellular activity of siRNA.[14] The tricyclic cytosine family (tC, tC°),[15] the quadracyclic adenosine family (*e.g.* qAN1, qAN4, 2CNqA)[16] and pentacyclic adenosine (pA)[17] with more red-shifted absorption maxima (350–387 nm) and improved brightness inside nucleic acid sequences (true for tC, tC°, 2CNqA and pA) have found interesting applications in

[a] Dr. H.-N. Le,[+] Dr. J. Kuchlyan,[+] Prof. B. Albinsson, Prof. L. M. Wilhelmsson
Department of Chemistry and Chemical Engineering
Chalmers University of Technology
Kemivägen 10, SE-41296 Gothenburg, Sweden.
E-mail: marcus.wilhelmsson@chalmers.se

[b] Dr. H.-N. Le,[+] Dr. T. Baladi, Dr. A. Dahlén
Cell Gene and RNA Therapy, Discovery Science
BioPharmaceuticals R&D, AstraZeneca
Pepparedsleden 1, 431 50 Gothenburg, Sweden
E-mail: anders.dahlen@astrazeneca.com

[+] These authors contributed equally

Supporting information for this article is available on the WWW under https://doi.org/10.1002/chem.202303539

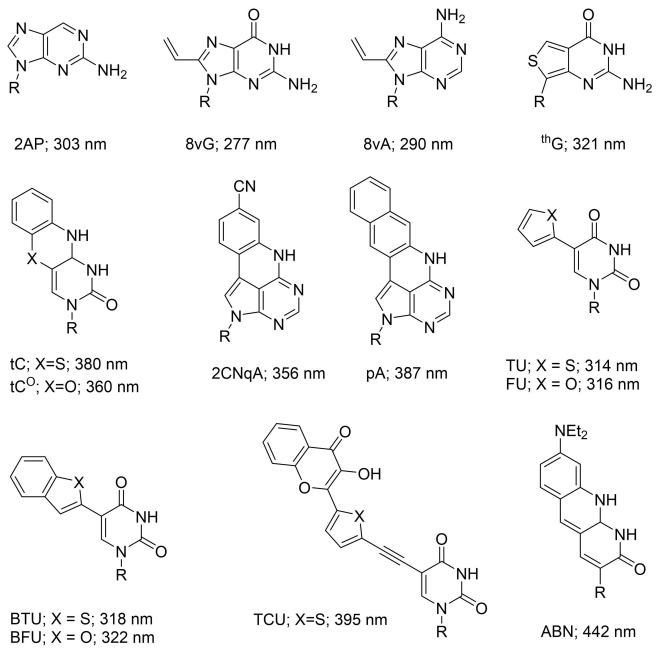

Figure 1. Structures and wavelength of absorption maxima of a selection of well characterized FBAs. R denotes the nucleic acid sugar which is ribose or 2′-deoxyribose. Absorption maxima reported are measured in aqueous solution.

sensing nucleic acids structure and in cellular imaging.[3a] Recently, tC, tC°, 2CNqA, and pA were utilized to label antisense oligonucleotide (ASO) gapmers with encouraging results.[3a] Moreover, tC° has recently shown great potential as a minimally perturbing label for therapeutic mRNA uptake studies in living cells as demonstrated by the in-cell translation of tC°-labeled mRNA into a functional protein.[3b] Also, other fluorescent base analogues have recently been reported to be read by natural enzymes,[18] where the application for metabolic fluorescence labelling reported by Kleiner *et al.* is a prominent example.[19]

In the last few decades, significant efforts have also led to a number of thymine or uracil FBAs.[20] For example, furan-modified uracil (FU, λ_{max} 316 nm) and thiophene-modified uracil (TU, λ_{max} 314 nm) are FBAs with environment sensitivity and that can be incorporated into DNA and RNA oligonucleotides without affecting the native structures.[21] FU has found interesting applications in probing the polarity of the micro-environment of nucleic acid helix grooves as well as mismatch detection. The same FBA also showed remarkable fidelity in enzymatic incorporation.[22] A similar approach has led to the development of a family of 5-modified thymine analogues.[23] Among them, the benzofuran-modified uracil (BFU) represents an excellent real-time reporter of enzymatic activity of DNA polymerase by following its incorporation into DNA.[23a] Recently, single and dual emissive analogues of thymine were developed for FRET application, sensing DNA hydration and conformation.[24] These FBAs (TCU, FCU) demonstrate excellent absorptivity in the visible region (ca. 40.000 $cm^{-1}M^{-1}$) with moderate QYs in water. When incorporated into DNA, these FBAs showed only a slight decrease in melting temperature with an excellent ratio-metric response; however, they showed fairly low and sequence-dependent QYs.[24a,b] More recently, an extremely bright thymine analogue (ABN) for single molecule detection of DNA was reported.[25] ABN has excellent brightness and absorption in the visible region. However, ABN introduced a significant destabilization for certain duplex sequences (ΔT_m as low as −14 °C for short oligonucleotides) and low base-pairing selectivity. Moreover, those bright FBAs displaying absorption in the visible region of the spectrum (TCU, FCU, ABN) have so far only been developed for labelling of DNA oligonucleotides. Hence, further development toward bright, red-shifted, FBAs which faithfully mimic uracil for RNA labelling is needed. Combining these characteristics with pH sensitivity that can help probe the local environment of the therapeutic nucleic acid upon uptake and trafficking inside the cell would be highly valuable.

Herein, we report the synthesis and photophysical characterization of a new FBA – quadracyclic uracil (qU, Figure 2). qU was designed to form a Watson-Crick base pair with adenine by keeping the hydrogen-bond capacity and, hence, to have a minimal effect on RNA structure and dynamics upon U to qU exchanges. We report on and discuss different synthetic routes towards the qU nucleobase and ribonucleoside. In our photophysical characterization of qU we found evidence of an equilibrium between two tautomeric forms being present in aqueous solution at ambient temperature – an iminol and an amide form and found that qU has absorption in the visible region and a high brightness. We also found that qU has two distinct emission bands, in part associated with the tautomers mentioned above, having a maximum at 440 nm and 530 nm, respectively. Interestingly, qU has pH-sensitive absorption and emission profiles as well as lifetimes which may prove useful for probing pH of various environments in live-cell imaging.

Results and Discussion

Retrosynthetic analysis

Design and retrosynthetic analysis of qU analogue led to two possible synthetic routes (Figure 2). In theory, qU can be obtained from the corresponding chloro derivative **4** in route (a), which can be disconnected further at the C–C bond on ring C leading to easily accessible intermediates **2a**–**e**. Compounds **2a**–**e** can then be synthesized through S_NAr reaction between the isoquinoline derivative **1** and appropriate phenols. Alternatively, qU can also be disconnected according to route (b), where the C–O bond on ring C is cut. The synthetic route was

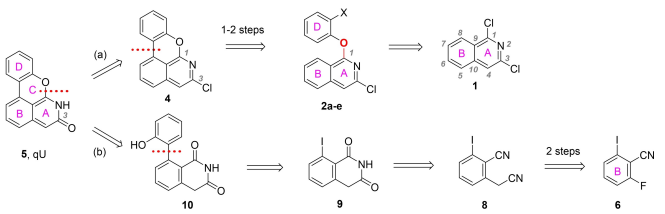

Figure 2. Design and retrosynthetic analysis of qU nucleobase.

inspired by a procedure developed by Wang *et al.*, for the synthesis of isoquinoline-1,3-diones from dinitriles.[26] We envisioned that the last step (ring C formation) of this synthetic route is a key step and could be challenging. Therefore, route (a) was first pursued due to fewer required steps for this option.

Synthesis of the qU nucleobase

Initially, the qU FBA was synthesized via a 4-step procedure (Figure 3a) starting from 1,3-dichloroisoquinoline (**1**). An S_NAr reaction between compound **1** and 2-aminophenol provided amine **2a** with excellent regioselectivity and chemoselectivity, confirmed by NMR. This is in line with literature precedence of haloselectivity on the isoquinoline ring, in which position 1 reacts much faster than position 3 (Figure 2).[27] Next, the tetracyclic fused heterocycle **4** was obtained through a 2-step, 1-pot process involving diazotization and copper-catalyzed intramolecular cyclization, known as a Pschorr reaction.[28] The conversion of amine **2** to the corresponding diazonium salt **3** was straightforward with above 95% conversion. Meanwhile, the Pschorr reaction was not very efficient affording mainly deaza compound as the main product and only 10% of the desired product **4**. Therefore, this was a bottleneck of the overall route in terms of scalability and yield (10%, 2 steps). In the last step, qU was obtained from compound **4** by replacement of the chloro functionality at position 3 with a hydroxyl group followed by a keto-enol tautomerization. It is noteworthy to mention that qU can have two main tautomeric forms (Figure S2), which is similar to several other FBAs.[25,29] An attempt to employ an S_NAr reaction (using NaOH or KOH in DMSO) was unsuccessful. The second approach using Pd_2dba_3 catalyst and Me_4tButylXPhos ligand (developed by Buchwald *et al.*)[30] proved successful and provided the product but in a low yield (11%). Overall, a limited amount but enough material with high purity was obtained for a preliminary photophysical characterization (data not shown) that motivated us to push towards the development of the qU nucleoside.

Several synthetic routes were investigated during the optimization of the qU nucleobase (Figure S3). Those routes relied on intramolecular C–C bond formation (Figure 2–route (a)) catalyzed by $FeCl_3$,[31] Pd-catalyst,[32] or Cu[28] without favorable outcome. Indeed, route (a) disconnection suffered from base–labile C1–O bonds forming after the first S_NAr reactions and inefficient C–C bond formation during the ring-closure step. The C1–O bond's instability can be explained by the fact that strong nucleophilic bases (such as KOH and NaOH) can attack at the C1 position on the isoquinoline ring in an S_NAr fashion. The S_NAr reaction is favored due to the highly nucleophilic nature at the C1 position and the formation of phenolate product as a good leaving group. Hence, route (a) disconnection was not favored at the latter stage of our project.

Utilizing the retrosynthetic route set out in Figure 2–route (b), compound **8** was synthesized from **6** via a 2-step procedure (Figure 3b) developed by Wang *et al.*[26] Herein, we modified the workup procedures so that no column chromatography was required. Compound **7** was purified by precipitation from acetone/water and compound **8** was isolated simply by precipitation from water. Moreover, higher yields were obtained for both reactions.

From dinitrile **8**, treatment with conc. HCl to form **9**[26] followed by Suzuki cross-coupling to obtain intermediate **10** and C–O bond formation led to the desired product **qU**. This procedure requires three more synthetic steps where we envisioned that the last step may have similar reaction conditions as the first one. Hence, by slightly modifying the order of reactions, we could reduce the number of steps required for this synthetic route. Indeed, Suzuki cross coupling between dinitrile **8** and (2-hydroxyphenyl)boronic acid was straightforward and high-yielding. After all the volatiles had been removed, the crude reaction mixture was treated with conc. HCl to provide the desired product **qU**. Interestingly, starting with only ring B on dinitrile **8**, ring D could be introduced by Suzuki cross coupling and then spontaneously forming ring C and ring A in the same pot. Moreover, qU was isolated from the reaction mixture by precipitation from water with 98% yield over 2 steps. The product isolated by this method was around 80–85% LC/MS purity, which could be used directly for the next glycosylation step. In fact, qU has limited solubility in common solvents which disfavored its purification by column chromatography. A small amount of product was recrystallized from DMSO/water and then DMSO/heptane for NMR characterization.

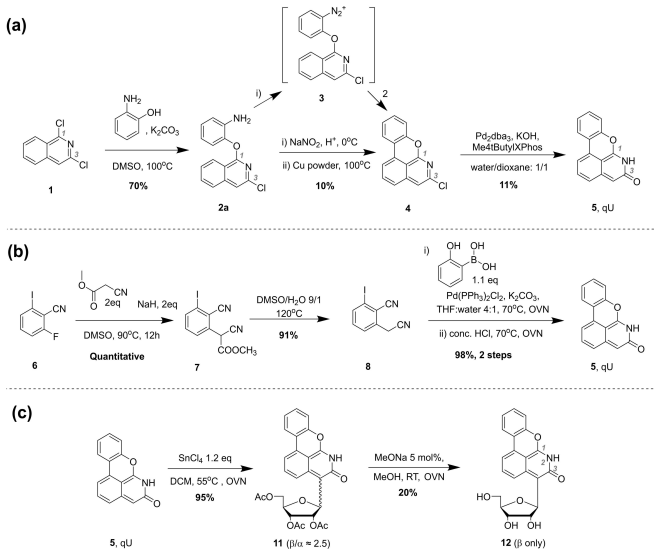

Figure 3. Synthesis of the qU nucleobase (a) and (b) and qU ribonucleoside (c).

Synthesis of the qU ribonucleoside

With a significant amount of the qU nucleobase at hand, we explored the chemistry further (Figure 3c) to synthesize the ribonucleoside version of qU (**12**). Compound **11** was synthesized from qU (**5**) through an acid catalyzed Friedel-Crafts reaction. The reaction likely happens through a Fries-type rearrangement[33] in which the sugar part is first connected to

the oxygen at position 3 of the isoquinoline ring and then rearranged to form the C-glycosylation product. Both the α- and β-anomers were formed with a β/α ratio of ca. 2.5 as estimated by LC/MS. These diastereoisomers eluted closely on TLC and were difficult to separate using normal-phase column chromatography. Therefore, a mixture of both anomers was carried over to the next step, in which the acetyl groups were removed under a catalytic amount of NaOMe in MeOH to provide the desired qU ribonucleoside **12**. Selective NOESY at 5.43 ppm (corresponding to H-1′) was used to confirm the stereochemistry at position 1′ on the ribose sugar. Indeed, H-1′, H-4′ correlation indicated that the isolated compound had the desired β conformation. To our surprise, 13 C-NMR spectral analysis of compound **12** showed that the iminol form (Figure S2) is dominant in DMSO-d_6. The product of this step was isolated in low yield mainly due to purification difficulties in separating the two diastereoisomers and of low solubility of the qU nucleoside product. However, the overall yield of the synthesis provided us with ample qU ribonucleoside for a detailed photophysical characterization.

Photophysical characterization of the qU ribonucleoside

Next, we performed a photophysical characterization of the qU ribonucleoside. As mentioned, the NMR characterization after synthesis of the target compound suggested that qU exists predominantly in its iminol tautomeric form (see Figure 7 below), *i.e.* with the hydrogen residing on the carbonyl oxygen rather than on the nitrogen (amide form; see Figure 7 and Figure S2). In our photophysical analysis presented here we find evidence of the same. First, qU was investigated for its photophysical properties in aqueous solution at varying pH (pH 3 to 12). At pH 7 qU has an absorption spectrum with a maximum at 380 nm with a molar absorptivity of 9600 $M^{-1}\,cm^{-1}$ (Figure 4). As pH was changed, the absorption of qU showed significant variation in spectral features (Figure 4). The absorption maximum appears at 380 nm at acidic as well as neutral pH (pH 3, pH 5, and pH 7) with a longer wavelength shoulder at around 450 nm. At higher pH (8–12) qU undergoes an absorption maximum red shift which shows the strong influence on the absorption by pH. From the spectra in Figure 4 it is also evident that the shoulder at around 450 nm, which is present at acidic and neutral pH, disappears under basic conditions. We have performed experiments at other qU concentrations where we see no significant changes (data not shown) from the spectra reported here which rules out the possibility of a considerable stacking between qU monomers in solution. The spectra show features that are close to being isosbestic points, for example, around 450 and slightly above 400 nm. The lack of perfect isosbestic points in this pH titration strongly suggests the existence of three rather than two species, namely the amide, iminol, and deprotonated anionic form of qU (Figure 7). It has been established in previous studies that the amide form of chromophores with structure features like qU generally absorbs at longer wavelength than the corresponding iminol form.[34] Moreover, we have performed quantum chemical calculations showing the same trend. The lowest lying absorption peak of the amide form is predicted at approximately 70 nm longer wavelengths than the corresponding iminol (see Supporting information 4). Hence, the presence of a small 450 nm peak and a stronger 380 nm peak at acidic and neutral pH suggests that qU under those conditions exists in equilibrium between its amide and iminol forms with the iminol as the dominating one. At basic pH (10–12; pH 11 omitted in Figure 4 to avoid a too busy graph) qU is deprotonated resulting in disappearance of the iminol and amide peaks mentioned above and instead an absorption peak at 408 nm originating from the anionic iminol species (Figure 7). We also note that there is no evidence of this peak below pH 5 (Figure 4) meaning, as expected, that the anionic form is not present under mildly acidic conditions. From previous literature on similar chromophores, we suggest that the deprotonation of the qU nucleoside leads to the negative charge being localized to the oxygen of the iminol form of qU.[34b,35] For determination of pK_a we used the shoulder of the absorption peak at 397 nm present at low pH and the 408 nm peak originating from the anionic iminol form at higher pH. From this absorption titration we have calculated the pK_a of the qU nucleoside to be ~8.8 (Figure 4).[34a] We also measured the excitation spectra of qU at

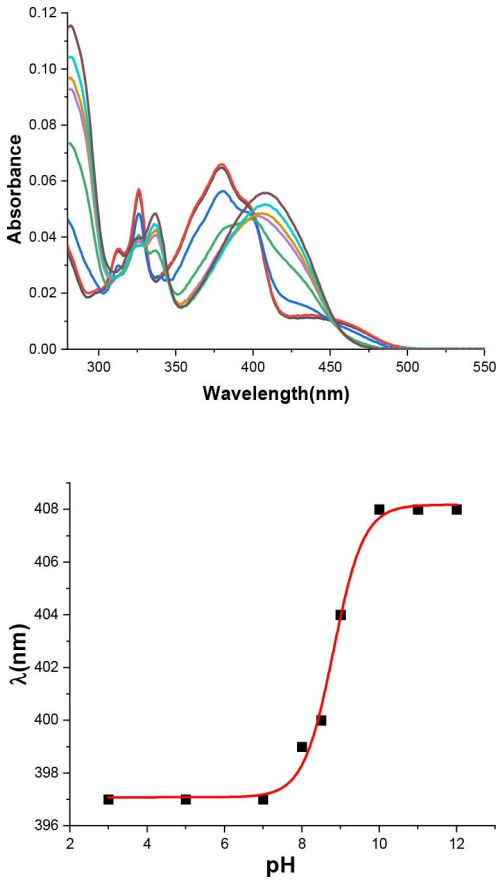

Figure 4. (Top) The absorption spectra of qU nucleoside at various pHs (pH 3, black; pH 5, red; pH 7, blue; pH 8, green; pH 8.5, violet; pH 9, dark yellow; pH 10, cyan; pH 12, wine). (Bottom) Correlating absorption wavelength to pH shows one major transition with inflection point. The experimental points (black disks) were fitted (red curve) to estimate pK_a.

various pHs monitored at the emission peak at 530 nm (see details of the emission features below) and they show similar features as the normal absorption spectra (Figure S4). As a final investigation of the absorptive properties of qU, we performed measurements in a series of less polar solvents. In all of these (DMSO, ethanol, methanol, dioxane, and acetonitrile) the peak at 450 nm, which is present in aqueous solution, is lacking (Figure S5). In the quantum chemical calculations of the iminol and amide form of qU the energy difference between the amide and iminol is significantly higher in less polar solvent compared to in water (see Supporting information Table S1). This would further push the balance towards the iminol form, again strongly suggesting that the 450 nm peak belongs to the amide tautomeric form of qU. It is worth noting that for correct base pairing with A, qU needs to be in its amide form. Whereas we have found that the iminol form is the dominant one as a monomer in aqueous solution it is not unlikely in RNA sequences that the presence of an A in the opposite strand will push the equilibrium towards more of the amide form resulting in correct base pairing with A. In previous studies of our tricyclic cytosines, tC and tC°, we have found that depending on which nucleobase is presented in the pairing position to the C-analogues they can exist in both tautomeric forms under otherwise similar conditions.[36] Future studies from our lab involving measurements of qU inside RNA-sequences will unveil these aspects further.

The fluorescence spectra of the qU nucleoside also exhibit significant pH dependence (Figure 5). The emission spectrum of qU at neutral pH has a distinct dual-band character with one peak centered around 440 nm and the other one around 530 nm (Figure 5). These bands are also pronounced in acidic pH and to some extent present also at slightly basic solutions (up to pH 9; Figure 5). With increasing pH (3 to 9) the intensity of the band centered around 440 nm decreases. This is also true for the 530 nm band which on the other hand gets increasingly dominating overall in the emission spectrum, *i.e.* its contribution to the overall qU emission/QY increases with pH. At high pHs, where the anionic form of qU dominates, the 530 nm band is dominating or occurs as a single band. From measurements that we performed in different organic solvents such as methanol, ethanol, DMSO, dioxane, and acetonitrile the qU chromophore seems to be essentially insensitive to the solvent polarity (Figure S5). No change of the emission peak maximum was observed except for a slight (4 nm) redshift in DMSO. Also, it is worth noting that the broad long-wavelength peak at 530 nm is completely absent in the various organic solvents used in the investigation (Figure S5). Moreover, it is interesting to note that the 530 nm band is present even at acidic pHs where the anionic ground state form is not present (Figure 4). Below we provide evidence indicating that the emission originating from both the amide and anionic species exhibit closely aligned spectral features and a maximum around 530 nm. From the absorption titration above we concluded that the amide form of qU is present as a minor species at neutral and acidic pH. By exciting in the region where the amide is the solitary contribution to absorption at these pH conditions (450 nm and above) we get an emission that has a peak at around 530 nm (Figure S6). Hence, we suggest that the 530 nm peak of the dual emission band character that we observe here for qU in aqueous solutions under non-basic conditions is at least partly related to emission from the amide form (Figure 7). Moreover, as will be more obvious from the time-resolved experiments below, we suggest that an excited state proton transfer (ESPT) process, which is a fundamental reaction in chemistry and biology[24c,37] also contributes to the 530 nm band at neutral and acidic pH.

ESPT has previously been reported for many chromophores/fluorophores and occurs by a photoexcited neutral form of a molecule undergoing proton transfer in the excited state to generate a tautomer and/or ionic form, resulting in a dual fluorescence band (Figure 5).[24c,38] In our case the qU nucleoside shows dual bands between pH 3 and 9 not only as an effect the main iminol band at 440 nm and amide band at 530 nm but also as an effect of the neutral, uncharged iminol form undergoing proton transfer to the solvent in the excited state to form the corresponding excited state anionic species. The emission from the anionic form contributes to the red-shifted emission peak at around 530 nm that is also found, but as a single peak, at high pHs in which the excited state anionic species is formed without ESPT. It is worth noting that qU does not show evidence of ESPT or the amide form in less polar/protic solvents (methanol, ethanol, DMSO, dioxane, acetonitrile; Supporting information Figure S5) since no broad emission peak at longer wavelength (530 nm) occurs under those conditions. This is not unexpected since it has been found

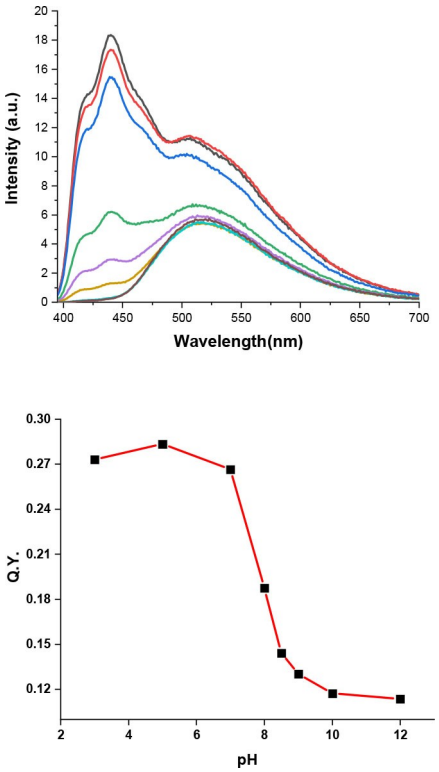

Figure 5. (Top) Emission spectra of qU recorded at different pH (pH 3, black; pH 5, red; pH 7, blue; pH 8, green; pH 8.5, violet; pH 9, dark yellow; pH 10, cyan; pH 12, wine), (bottom) Emission QY vs pH plot.

Table 1. Time-resolved data of qU at different pH monitored at 440 nm.

	τ_1 /ns	a_1	τ_2 /ns	a_2	τ_3 /ns	a_3	$<\tau>$ /ns
pH 3	0.65	0.56	2.81	0.20	5.51	0.23	2.24
pH 5	0.54	0.55	2.71	0.22	5.11	0.22	2.04
pH 7	0.65	0.56	3.02	0.20	6.22	0.23	2.44
pH 8	0.61	0.59	3.02	0.20	5.74	0.20	2.16

Table 2. Time-resolved data of qU at different pH monitored at 530 nm.

	τ_1 /ns	a_1	τ_2 /ns	a_2	τ_3 /ns	a_3	$<\tau>$ /ns
pH 3	0.65	−0.26			5.08	0.74	3.92
pH 5	0.65	−0.23			5.1	0.76	4.05
pH 7	0.53	−0.23			5.33	0.77	4.24
pH 8	0.48	−0.15			5.31	0.84	4.56
pH 10			4.75	0.80	6.98	0.20	5.19
pH 12			4.77	0.81	8.39	0.19	5.47

previously that water plays a vital and unique role for proton transfer processes where it has an active role in deprotonation, stabilization of the ion pair formed after proton transfer, and transport mechanism of the protons.[37]

As an effect of this existence of different emissive species, the quantum yield (QY) of qU varies with pH (Figure 5). The QY of qU at neutral and acidic pH is 0.27 ± 0.02 (resulting in a brightness, $\varepsilon \times \Phi_{fr}$ of approximately 2600 $M^{-1}cm^{-1}$, which is higher than the previously reported and promising U-analogues ^{th}U, 1300 $M^{-1}cm^{-1}$,[10] and TPAU, 2200 $M^{-1}cm^{-1}$)[39] and decreases rapidly between pH 7 and 9 where the emissive species that give rise to the 440 nm band vanishes fast. At high pH where only the 530 nm-band species is present the QY was measured to 0.12 (Figure 5). This band and emission QY originate from the anionic species suggested in Figure 7.

To further investigate the nature of the different species of the qU nucleoside in the excited state and give more conclusive evidence of the ESPT reaction we performed fluorescence lifetime measurements. In a time-correlated single-photon counting (TCSPC) study, we monitored the emission band centered at 440 nm and the red-shifted band at 530 nm, respectively. The lifetime data from monitoring at 440 and 530 nm are shown in Table 1 and 2, respectively, and the corresponding fluorescence decay curves are depicted in Figure 6. We found that the time-resolved decays are best fitted with a triexponential function when monitored at 440 nm and a biexponential ditto at 530 nm. When we monitored the blue-shifted band a fast time component (~540–650 ps) was observed as the major contribution (the pre-exponential factor of τ_1, a_1, is larger than a_2 and a_3). The other two-time components (τ_2 = 2.71–3.02 ns and τ_3 = 5.11–6.22 ns, respectively) contribute to an almost equal amount (a_2 and a_3 are all between 20 and 23%). The three lifetimes needed to fit the 440 nm decays are difficult to assign to single species. However, having ESPT reactions that in principle could be in equilibrium would give contributions to the decays from both the iminol proton donor and the two possible products. Hence, a possible assignment would be that the fast decay (~600 ps) is from the iminol proton donor and the two nanosecond decays from the anionic and tautomer amide forms. When instead monitoring the red-shifted band at 530 nm we observed a negative amplitude (15–26%) with a fast time component (~480–650 ps) similar to the fast decay component at 440 nm. This rise-time component is only present in samples between pH 3 and 8 where the amount of the anionic form in ground state (Figure 7) is negligible and the ESPT processes discussed above can be expected to occur. We found that the percentage of the rise component is between 23 and 26% for pH 3–7 decreasing to 15% for pH 8. For these low and neutral pHs we observed a single, slow decay time component of slightly above 5 ns (5.10–5.31 ns) with an amplitude varying between 74 and 84%. On the contrary, at the basic pHs monitored in the study (10 and 12) two time components of 4.75–5.34 ns with an amplitude of approximately 80% and 6.98–8.39 ns with an amplitude of approximately 20% were observed. Under these conditions there was no sign of a rise-time component.

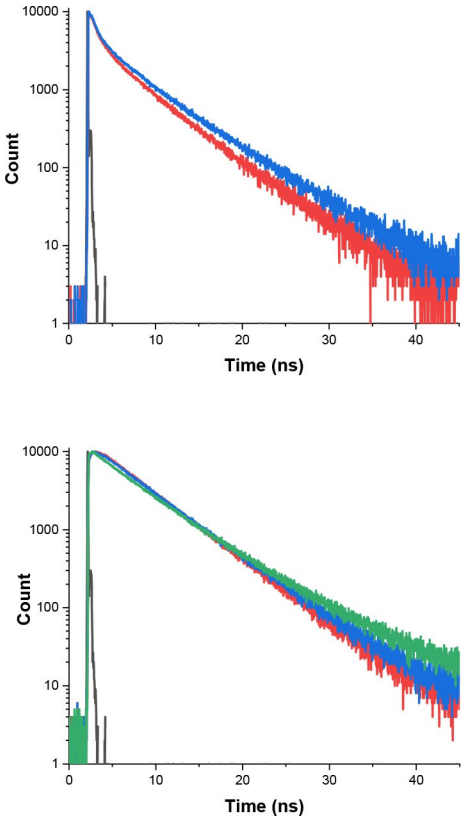

Figure 6. (Top) Fluorescence decays recorded at pH 3 (red) and 7 (blue). Excitation and emission wavelengths were at 380 nm and 440 nm, respectively. (Bottom) Fluorescence decays recorded at pH 3 (red), 7 (blue), and 12 (green). Excitation and emission wavelengths were at 380 nm and 530 nm, respectively. Black lines are the IRF profile.

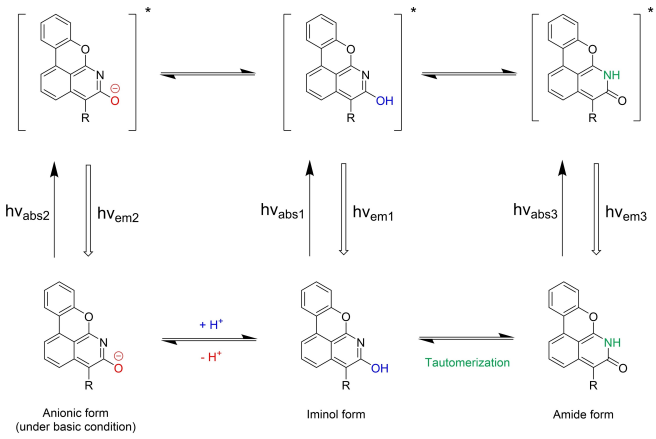

Figure 7. Ground- and excited state species of qU. The wavelengths of absorption maxima for the lowest energy transitions of the three cases: $abs_1 = 380$ nm; $abs_2 = 408$ nm; $abs_3 = 450$ nm. Corresponding values for emission maxima: $em_1 = 440$ nm; $em_2 = 530$ nm; $em_3 = 530$ nm.

Conclusions

Here we present and discuss two synthetic routes towards the new ribonucleoside analogue qU. We have also in detail photophysically characterized the qU ribonucleoside and found it to be fluorescent with a quantum yield of 27% at neutral and acidic pH. We report on a dual-band emission in the pH range 3 to 9 resulting from an ESPT reaction and that the dual-band character varies significantly with pH. With its high brightness, absorption in the visible region, and pH sensitivity, this new fluorescent base analogue extends the toolbox of native-like RNA labels. Ongoing investigations involve incorporation of qU into RNA sequences and understanding its photophysics inside RNAs. The detailed steady-state and time-resolved photophysical characterization performed here paves the way, for example, for future applications of this label in live-cell confocal and fluorescence lifetime imaging (FLIM) of RNA therapeutics where qU's pH sensitivity may be applied to probe the microenvironment around the RNA.

Supporting Information

The authors have cited additional references within the Supporting Information.[40]

Acknowledgements

This work was conducted as part of the FoRmulaEx research center for nucleotide delivery and with associated financial support to L. M. W. from the Swedish Foundation for Strategic Research (SSF, grant No. IRC15-0065). We thank Dr. Thanh Nguyen (AstraZeneca) for fruitful discussion on the synthesis of qU nucleobase and Mr. Rasmus Ringström for valuable discussions regarding the photophysics of qU.

Conflict of Interests

The authors declare no conflict of interest.

Data Availability Statement

The data that support the findings of this study are available from the corresponding author upon reasonable request.

Keywords: dual emission · FBA · fluorescence · pH sensitivity · uridine analog

[1] a) C. He, M. T. Migawa, K. Chen, T. A. Weston, M. Tanowitz, W. Song, P. Guagliardo, K. S. Iyer, C. F. Bennett, L. G. Fong, P. P. Seth, S. G. Young, H. Jiang, *Nucleic Acids Res.* **2020**, *49*, 1–14; b) K. Deprey, N. Batistatou, M. F. Debets, J. Godfrey, K. B. VanderWall, R. R. Miles, L. Shehaj, J. Guo, A. Andreucci, P. Kandasamy, G. Lu, M. Shimizu, C. Vargeese, J. A. Kritzer, *ACS Chem. Biol.* **2022**, *17*, 348–360; c) E. Kay, R. Stulz, C. Becquart, J. Lovric, C. Tängemo, A. Thomen, D. Baždarević, N. Najafinobar, A. Dahlén, A. Pielach, J. Fernandez-Rodriguez, R. Strömberg, C. Ämmälä, S. Andersson, M. Kurczy, *Pharmaceutica* **2022**, *14*; d) T. Gökirmak, M. Nikan, S. Wiechmann, T. P. Prakash, M. Tanowitz, P. P. Seth, *Trends Pharmacol. Sci.* **2021**, *42*, 588–604; e) M. J. Munson, G. O'Driscoll, A. M. Silva, E. Lázaro-Ibáñez, A. Gallud, J. T. Wilson, A. Collén, E. K. Esbjörner, A. Sabirsh, *Communications Biology* **2021**, *4*, 211.
[2] a) M. Levitus, S. Ranjit, *Q. Rev. Biophys.* **2011**, *44*, 123–151; b) S. Lorenz, S. Tomcin, V. Mailänder, *Microscopy and microanalysis: the official journal of Microscopy Society of America* Microbeam Analysis Society, Microscopical Society of Canada **2011**, *17*, 440–445.
[3] a) J. R. Nilsson, T. Baladi, A. Gallud, D. Baždarević, M. Lemurell, E. K. Esbjörner, L. M. Wilhelmsson, A. Dahlén, *Sci. Rep.* **2021**, *11*, 11365; b) T. Baladi, J. R. Nilsson, A. Gallud, E. Celauro, C. Gasse, F. Levi-Acobas, I. Sarac, M. R. Hollenstein, A. Dahlén, E. K. Esbjörner, L. M. Wilhelmsson, *J. Am. Chem. Soc.* **2021**, *143*, 5413–5424.
[4] A. Lacroix, E. Vengut-Climent, D. de Rochambeau, H. F. Sleiman, *ACS Cent. Sci.* **2019**, *5*, 882–891.
[5] a) W. Xu, K. M. Chan, E. T. Kool, *Nat. Chem.* **2017**, *9*, 1043–1055; b) B. Y. Michel, D. Dziuba, R. Benhida, A. P. Demchenko, A. Burger, *Front. Chem.* **2020**, *8*, 112; c) L. M. Wilhelmsson, *Q. Rev. Biophys.* **2010**, *43*, 159–183.
[6] D. C. Ward, E. Reich, L. Stryer, *J. Biol. Chem.* **1969**, *244*, 1228–1237.
[7] M. Bood, S. Sarangamath, M. S. Wranne, M. Grøtli, L. M. Wilhelmsson, *Beilstein J. Org. Chem.* **2018**, *14*, 114–129.
[8] A. Nadler, J. Strohmeier, U. Diederichsen, *Angew. Chem. Int. Ed.* **2011**, *50*, 5392–5396.
[9] N. Ben Gaied, N. Glasser, N. Ramalanjaona, H. Beltz, P. Wolff, R. Marquet, A. Burger, Y. Mély, *Nucleic Acids Res.* **2005**, *33*, 1031–1039.
[10] D. Shin, R. W. Sinkeldam, Y. Tor, *J. Am. Chem. Soc.* **2011**, *133*, 14912–14915.
[11] a) J. Kuchlyan, L. Martinez-Fernandez, M. Mori, K. Gavvala, S. Ciaco, C. Boudier, L. Richert, P. Didier, Y. Tor, R. Improta, Y. Mély, *J. Am. Chem. Soc.* **2020**, *142*, 16999–17014; b) V. Kilin, K. Gavvala, N. P. F. Barthes, B. Y. Michel, D. Shin, C. Boudier, O. Mauffret, V. Yashchuk, M. Mousli, M. Ruff, F. Granger, S. Eiler, C. Bronner, Y. Tor, A. Burger, Y. Mély, *J. Am. Chem. Soc.* **2017**, *139*, 2520–2528.
[12] S. Park, H. Otomo, L. Zheng, H. Sugiyama, *Chem. Commun.* **2014**, *50*, 1573–1575.
[13] M. Sholokh, R. Sharma, N. Grytsyk, L. Zaghzi, V. Y. Postupalenko, D. Dziuba, N. P. F. Barthes, B. Y. Michel, C. Boudier, O. A. Zaporozhets, Y. Tor, A. Burger, Y. Mély, *Chem. - Eur. J.* **2018**, *24*, 13850–13861.
[14] D. Shin, P. Lönn, S. F. Dowdy, Y. Tor, *Chem. Commun.* **2015**, *51*, 1662–1665.
[15] a) S. Preus, K. Kilså, L. M. Wilhelmsson, B. Albinsson, *Phys. Chem. Chem. Phys.* **2010**, *12*, 8881–8892; b) B. Dumat, A. F. Larsen, L. M. Wilhelmsson, *Nucleic Acids Res.* **2016**, *44*, e101-e101; c) A. F. Füchtbauer, S. Preus, K. Börjesson, S. A. McPhee, D. M. J. Lilley, L. M. Wilhelmsson, *Sci. Rep.* **2017**, *7*, 2393; d) K.-Y. Lin, R. J. Jones, M. Matteucci, *J. Am. Chem. Soc.* **1995**, *117*, 3873–3874.
[16] a) A. Wypijewska del Nogal, A. F. Füchtbauer, M. Bood, Jesper R. Nilsson, M. S. Wranne, S. Sarangamath, P. Pfeiffer, V. S. Rajan, A. H. El-Sagheer, A.

Dahlén, T. Brown, M. Grøtli, L. M. Wilhelmsson, *Nucleic Acids Res.* **2020**, *48*, 7640–7652; b) B. Dumat, M. Bood, M. S. Wranne, C. P. Lawson, A. F. Larsen, S. Preus, J. Streling, H. Gradén, E. Wellner, M. Grøtli, L. M. Wilhelmsson, *Chem. - Eur. J.* **2015**, *21*, 4039–4048.
[17] M. Bood, A. F. Füchtbauer, M. S. Wranne, J. J. Ro, S. Sarangamath, A. H. El-Sagheer, D. L. M. Rupert, R. S. Fisher, S. W. Magennis, A. C. Jones, F. Höök, T. Brown, B. H. Kim, A. Dahlén, L. M. Wilhelmsson, M. Grøtli, *Chem. Sci.* **2018**, *9*, 3494–3502.
[18] a) L. Dehmel, F. Berndt, M. Weinberger, M. Sajadi, I. Ioffe, H. A. Wagenknecht, N. P. Ernsting, *Phys. Chem. Chem. Phys.* **2016**, *18*, 6813–6820; b) M. Merkel, L. Dehmel, N. P. Ernsting, H.-A. Wagenknecht, *Angew. Chem. Int. Ed.* **2017**, *56*, 384–388.
[19] D. Wang, A. Shalamberidze, A. E. Arguello, B. W. Purse, R. E. Kleiner, *J. Am. Chem. Soc.* **2022**, *144*, 14647–14656.
[20] a) A. A. Tanpure, M. G. Pawar, S. G. Srivatsan, *Isr. J. Chem.* **2013**, *53*, 366–378; b) A. Fin, A. R. Rovira, P. A. Hopkins, Y. Tor, *in Modified Nucleic Acids* (Eds.: K. Nakatani, Y. Tor), Springer International Publishing, Cham, **2016**, pp. 1–26.
[21] a) N. J. Greco, Y. Tor, *Tetrahedron* **2007**, *63*, 3515–3527; b) A. J. Gutierrez, T. J. Terhorst, M. D. Matteucci, B. C. Froehler, *J. Am. Chem. Soc.* **1994**, *116*, 5540–5544.
[22] a) S. G. Srivatsan, Y. Tor, *Tetrahedron* **2007**, *63*, 3601–3607; b) S. G. Srivatsan, Y. Tor, *J. Am. Chem. Soc.* **2007**, *129*, 2044–2053; c) M. G. Pawar, S. G. Srivatsan, *Org. Lett.* **2011**, *13*, 1114–1117.
[23] a) P. Ghosh, H. M. Kropp, K. Betz, S. Ludmann, K. Diederichs, A. Marx, S. G. Srivatsan, *J. Am. Chem. Soc.* **2022**, *144*, 10556–10569; b) A. A. Tanpure, S. G. Srivatsan, *ChemBioChem.* **2012**, *13*, 2392–2399.
[24] a) K. Gavvala, N. P. F. Barthes, D. Bonhomme, A. S. Dabert-Gay, D. Debayle, B. Y. Michel, A. Burger, Y. Mély, *RSC Adv.* **2016**, *6*, 87142–87146; b) N. P. F. Barthes, K. Gavvala, D. Dziuba, D. Bonhomme, J. Karpenko, A. S. Dabert-Gay, D. Debayle, A. P. Demchenko, R. Benhida, B. Y. Michel, Y. Mély, A. Burger, *J. Mater. Chem. C* **2016**, *4*, 3010–3017; c) N. P. F. Barthes, J. Karpenko, D. Dziuba, M. Spadafora, J. Auffret, A. P. Demchenko, Y. Mély, R. Benhida, B. Y. Michel, A. Burger, *RSC Adv.* **2015**, *5*, 33536–33545; d) N. P. F. Barthes, K. Gavvala, D. Bonhomme, A. S. Dabert-Gay, D. Debayle, Y. Mély, B. Y. Michel, A. Burger, *J. Org. Chem.* **2016**, *81*, 10733–10741.
[25] G. N. Samaan, M. K. Wyllie, J. M. Cizmic, L.-M. Needham, D. Nobis, K. Ngo, S. Andersen, S. W. Magennis, S. F. Lee, B. W. Purse, *Chem. Sci.* **2021**, *12*, 2623–2628.
[26] J. Kankanala, C. Marchand, M. Abdelmalak, H. Aihara, Y. Pommier, Z. Wang, *J. Med. Chem.* **2016**, *59*, 2734–2746.
[27] A. D. Kharlamova, A. S. Abel, A. D. Averin, O. A. Maloshitskaya, V. A. Roznyatovskiy, E. N. Savelyev, B. S. Orlinson, I. A. Novakov, I. P. Beletskaya, *Molecules* **2021**, *26*, 1910.
[28] a) D. F. DeTar, *in Organomet. React.* pp. 409–462; b) H. Yin, W. Zhu, Y. Xu, M. Dai, X. Qian, Y. Li, J. Liu, *Eur. J. Med. Chem.* **2011**, *46*, 3030–3037.
[29] M. Sholokh, R. Improta, M. Mori, R. Sharma, C. Kenfack, D. Shin, K. Voltz, R. H. Stote, O. A. Zaporozhets, M. Botta, Y. Tor, Y. Mély, *Angew. Chem. Int. Ed.* **2016**, *55*, 7974–7978.
[30] K. W. Anderson, T. Ikawa, R. E. Tundel, S. L. Buchwald, *J. Am. Chem. Soc.* **2006**, *128*, 10694–10695.
[31] R. S. Jassas, E. U. Mughal, A. Sadiq, R. I. Alsantali, M. M. Al-Rooqi, N. Naeem, Z. Moussa, S. A. Ahmed, *RSC Adv.* **2021**, *11*, 32158–32202.
[32] a) L.-C. Campeau, M. Parisien, M. Leblanc, K. Fagnou, *J. Am. Chem. Soc.* **2004**, *126*, 9186–9187; b) I. B. Seiple, S. Su, R. A. Rodriguez, R. Gianatassio, Y. Fujiwara, A. L. Sobel, P. S. Baran, *J. Am. Chem. Soc.* **2010**, *132*, 13194–13196.
[33] a) H. Tachallait, M. Safir Filho, H. Marzag, K. Bougrin, L. Demange, A. R. Martin, R. Benhida, *New J. Chem.* **2019**, *43*, 5551–5558; b) R. G. dos Santos, A. R. Jesus, J. M. Caio, A. J. C. O. C. P. Rauter, *Curr. Org. Chem.* **2011**, *15*, 128–148.
[34] a) A. Matwijczuk, D. Karcz, R. Walkowiak, J. Furso, B. Gladyszewska, S. Wybraniec, A. Niewiadomy, G. P. Karwasz, M. Gagos, *J. Phys. Chem. A* **2017**, *121*, 1402–1411; b) Z. Xu, K.-H. Baek, H. N. Kim, J. Cui, X. Qian, D. R. Spring, I. Shin, J. Yoon, *J. Am. Chem. Soc.* **2010**, *132*, 601–610.
[35] A. Matwijczuk, D. Karcz, R. Walkowiak, J. Furso, B. Gładyszewska, S. Wybraniec, A. Niewiadomy, G. P. Karwasz, M. Gagoś, *J. Phys. Chem. A* **2017**, *121*, 1402–1411.
[36] G. Stengel, B. W. Purse, L. M. Wilhelmsson, M. Urban, R. D. Kuchta, *Biochemistry* **2009**, *48*, 7547–7555.
[37] N. Agmon, *Chem. Phys. Lett.* **1995**, *244*, 456–462.
[38] a) A. P. Demchenko, K.-C. Tang, P.-T. Chou, *Chem. Soc. Rev.* **2013**, *42*, 1379–1408; b) P. Zhou, K. Han, *Acc. Chem. Res.* **2018**, *51*, 1681–1690.
[39] R. W. Sinkeldam, P. A. Hopkins, Y. Tor, *ChemPhysChem.* **2012**, *13*, 3350–3356.
[40] a) K. Rurack, M. Spieles, *Anal. Chem.* **2011**, *83*, 1232–1242; b) M. J. Frisch, G. W. Trucks, H. B. Schlegel, G. E. Scuseria, M. A. Robb, J. R. Cheeseman, G. Scalmani, V. Barone, G. A. Petersson, H. Nakatsuji, X. Li, M. Caricato, A. V. Marenich, J. Bloino, B. G. Janesko, R. Gomperts, B. Mennucci, H. P. Hratchian, J. V. Ortiz, A. F. Izmaylov, J. L. Sonnenberg, Williams, F. Ding, F. Lipparini, F. Egidi, J. Goings, B. Peng, A. Petrone, T. Henderson, D. Ranasinghe, V. G. Zakrzewski, J. Gao, N. Rega, G. Zheng, W. Liang, M. Hada, M. Ehara, K. Toyota, R. Fukuda, J. Hasegawa, M. Ishida, T. Nakajima, Y. Honda, O. Kitao, H. Nakai, T. Vreven, K. Throssell, J. A. Montgomery Jr, J. E. Peralta, F. Ogliaro, M. J. Bearpark, J. J. Heyd, E. N. Brothers, K. N. Kudin, V. N. Staroverov, T. A. Keith, R. Kobayashi, J. Normand, K. Raghavachari, A. P. Rendell, J. C. Burant, S. S. Iyengar, J. Tomasi, M. Cossi, J. M. Millam, M. Klene, C. Adamo, R. Cammi, J. W. Ochterski, R. L. Martin, K. Morokuma, O. Farkas, J. B. Foresman, D. J. Fox, Wallingford, CT, **2016**.

Manuscript received: October 26, 2023
Accepted manuscript online: January 17, 2024
Version of record online: ■■, ■■

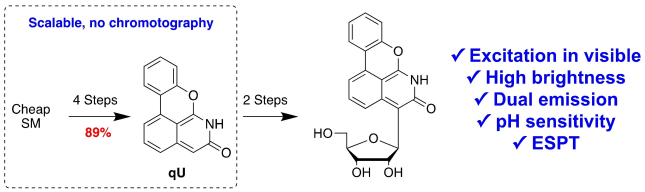

Dr. H.-N. Le, Dr. J. Kuchlyan, Dr. T. Baladi, Prof. B. Albinsson, Dr. A. Dahlén, Prof. L. M. Wilhelmsson**

1 – 9

Synthesis and photophysical characterization of a pH-sensitive quadracyclic uridine (qU) analogue

Herein, we present the synthesis and detailed photophysical characterization of qU – a novel fluorescent base analogue of uridine. qU exhibits interesting properties such as excitation in the visible region with high brightness, dual emission, pH sensitivity, and an ESPT reaction. This work has extended the toolbox of internal RNA labels for future applications such as fluorescence lifetime imaging.